Supplementary Information 2: Development of a Spatially Explicit Fate Factor Model at the 5 Arcmin Resolution

Contents

1 Methodology

1.1 Fate Factor Model Structure

FFs express the mass of nutrients in waterbodies (kg) per unit of emission per year (kg $year^{-1}$), yielding a time dimensional unit (year). As such, FFs describe the persistence fraction of the original nutrient emission (E) in the receiving waterbodies (w)[1].

For freshwater receptors (fw), the cumulative fate factor ($FF_{soils\ E\ (w)(z)(i)}$) for a soil emission in cell (i) of emission pathway, z (surface runoff, erosion or leaching) and nutrient type, E (Nitrogen (N) or Phosphorus (P)), is the product of nutrient soil emissions ($f_{E(z)(i)}$) to streams and the sum of the instream transportation of nutrients from cell (i) to all downstream freshwater receptor grid cells (j) ($\mathrm{f}_{\mathrm{E\ (i,j)}}$ dimensionless), divided by the rate of persistence in water in receptor cell j ($\lambda_{E(j)}$, $year^{-1}$); the ultimate downstream receptor cell j is the mouth (M) of the river system. $(FF_{E(fw)(i,j)})$[2]:

$$\mathrm{FF}_{\mathrm{soils\ E\ (fw)(z)\ (i)}} = f_{E(z)(i)} \sum_{\mathrm{j}} \mathrm{FF}_{\mathrm{River\ E(fw)(i,j)}} = f_{E(z)(i)} \sum_{\mathrm{j=i}}^{\mathrm{M}} \frac{\mathrm{f}_{\mathrm{E(i,j)}}}{\lambda_{\mathrm{E(fw)(j)}}}$$

All grid cells downstream of emission cell (i) are receptor cells (j) within freshwater environments. Therefore, for each downstream receptor cell (l being the receptor grid cell of focus) the fraction of downstream removal is multiplied by the product of all fractions of nutrients transported downstream $(1 - R_{E_l}); R = rentention)$ to the first upstream cell of receptor cell (j) (when the emission cell is also the receptor cell $\mathrm{f}_{\mathrm{E(fw)(z)(i,i)}} = 1$):

$$\mathrm{f}_{\mathrm{E(fw)(i,j)}} = \prod_{\mathrm{l=i}}^{\mathrm{j-1}} (1 - R_{E_l})$$

For marine receptors (LME), the cumulative fate factor is not considered and is the product of the fraction of soil emission $f_{E(z)(i)}$ and all subsequent instream transportation $\mathrm{f}_{\mathrm{E(i,j)}}$ from an emission in cell (i) until its receptor marine cell (j):

$$\mathrm{FF}_{\mathrm{soils\ E\ (LME)(z)\ (i)}} = f_{E(z)(i)} \frac{\mathrm{f}_{\mathrm{E(i,j)}}}{\lambda_{\mathrm{E(LME)(j)}}}$$

1.2 Nutrient Emission Fraction in Soil ($f_{E(z)(i)}$), and water($\mathrm{f}_{\mathrm{E(i,j)}}$)

The IMAGE-GNM model is the basis for estimating the nutrient emission fraction in soil ($f_{E(z)(i)}$) and water ($\mathrm{f}_{\mathrm{E(i,j)}}$) compartments of a cell. Studies have identified IMAGE-GNM as the most comprehensive option to develop FFs from soils[3,4]. IMAGE-GNM provides predictive advantages through detailed modelling of land fate processes rather than previous watershed lumped regression models (e.g. Global NEWS 2[5]), which have been used to develop previous FFs[6]. Additionally, IMAGE-GNM runs at the annual time-step which ties in with the preferred global and temporal scope of LCIA methodologies[4]; whereas, sub-annual (seasonal) temporal resolution models do not.

IMAGE-GNM model is coupled with PCR-GLOBWB[7] (a global hydrological model) to estimate global and spatially-explicit nutrient delivery of N and P to freshwater systems, via point and diffusive sources, at the 30 arcmin resolution[8]. Figure 1 shows a schematic of nutrient emission pathways from soils to rivers within each grid cell of IMAGE-GNM. Each cell has a land and water compartment; land compartments consider three emission pathways z (surface water runoff, erosion, leaching). The fraction of emission reaching receiving waterbodies undergoes processes such as denitrification within the riparian zone, soils and aquifers. Within water compartments, nutrients are removed under biological and chemical processes relating to denitrification, sedimentation and uptake by aquatic plants before being transported downstream to the next cell through advection.

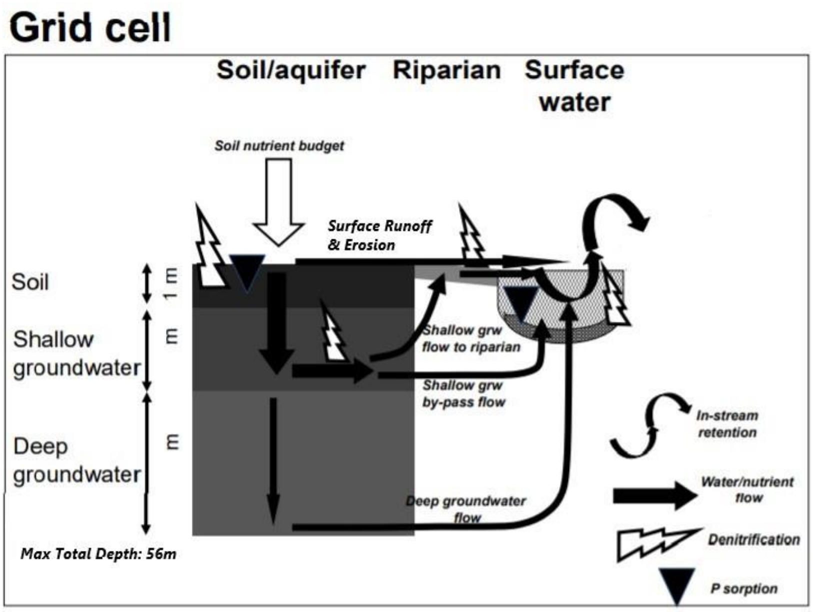

Figure 1: Adapted schematic diagram from Beusen et al., (2015) of soil emission flows to rivers.

This study uses IMAGE-GNM equations that transport and reduce nutrients within cells (($f_{E(z)(i)}$) and between cells ($f_{E(i,j)}$, dimensionless) to devise emissions from agricultural soils (Table 1). Whilst IMAGE GNM is written in Python, the FF model presented here is entirely written in MATLAB. We updated datasets used within IMAGE-GNM, which are now available for the 5 arcmin resolution (e.g. soil data[9], hydrographic information through PCR-GLOWBWB 2[10], aquifer thickness[11], porosity and permeability[12]), to tie in with our preferred 5 arcmin resolution of this study. Where datasets could not be updated (i.e., nutrient data modelled by IMAGE-GNM) we disaggregated, through an equal average, IMAGE-GNM datasets from 30 arcmin to 5 arcmin resolution. The datasets can be found in Appendix 1. The IMAGE-GNM equations that support the derived export fractions are described below and further details on the IMAGE-GNM methodology are presented by Beusen et al., (2015)[8] . All reduction factors can be found in Appendix 2.

Table 1: Inland Fate equations for N and P in receptor j.

Emission Route	Removal Fraction [-]	Derived equation for exported fraction*
Surface Runoff	$f_{Surface\ E\ (i)}$	$f_{qrso} \times R_{Subgrid}$
Erodibility	$f_{Erosion\ E\ (i)}$	$f_{ero} \times R_{Subgrid}$
Leaching – Shallow Groundwater flow to riparian	$f_{Leach,Shallow\ E\ (i)}$	$f_{leach,soil} \times f_{shallow,gw} \times f_{non-bypass} \times (1 - f_{den,rip}) \times R_{Subgrid}$
Leaching – Shallow Groundwater by-pass flow	$f_{Leach,Shallow\ E\ (i)}$	$f_{leach,soil} \times f_{shallow,gw} \times f_{bypass} \times f_{N,TS/SS} \times R_{Subgrid}$
Leaching – Deep Groundwater	$f_{Leach,Deep\ E\ (i)}$	$f_{leach,soil} \times f_{deep,gw} \times f_{N,TS/SS} \times R_{Subgrid}$
Leaching - Submarine Shallow Groundwater Discharge	$f_{Shallow,SGD\ (i)}$	$f_{leach,soil} \times f_{shallow,gw} \times f_{Shallow,SGD} \times R_{Subgrid}$
Leaching - Submarine Deep Groundwater Discharge	$f_{Deep,SGD\ (i)}$	$f_{leach,soil} \times f_{deep,gw} \times f_{Deep,SGD} \times f_{N,TS/SS} \times R_{Subgrid}$

* $f_{qrso}, f_{ero}, f_{leach,soil}$ relate to export fractions from surface water, erosion, and leaching; $f_{shallow,gw}, f_{deep,gw}$ indicate to export fractions within shallow and deep groundwater; $f_{Shallow,SGD}, f_{Deep,SGD}$ represent the fraction emitted directly to marine environments through submarine groundwater discharge; $f_{N,TS/SS}$ represent the reduction or increase fraction caused by historical fertiliser leaching; $f_{den,rip}$ is the denitrification fraction with riparian zones; $R_{Subgrid}$ is the subgrid retention factor in rivers solely.

1.2.1 Surface Runoff ($\boldsymbol{f_{qrso}}$)

$$f_{qrso} = f_{cal}(f_{qrso}(texture) f_{qrso}(slope) f_{qrso}(landuse))$$

$$f_{qrso}(slope) = 1 - e^{-0.00617 MAX[1,S]}$$

Where f_{qrso} is the surface runoff factor, f_{cal} is a correction coefficient of 0.3[13], S is the slope in m km^{-1}. f_{qrso} is reduced by $f_{qrso}(texture)$, $f_{qrso}(slope)$ and $f_{qrso}(landuse)$, for which their values can be found in Appendix 2 and described in Beusen et al., (2015)[8].

1.2.2 Erodibility ($\boldsymbol{f_{ero}}$)

The fraction of erodibility is determined by Cerdan et al., (2010)[14] to estimate soil loss by rainfall erosion:

$$f_{ero} = f_{ero}(slope) f_{ero}(texture)$$

$$f_{ero}(slope) = -1.5 + \frac{17}{1 + e^{2.3 - 6.1S}}$$

f_{ero} is the erodibility of soils influenced by the reduction factors of $f_{ero}(slope)$ and $f_{ero}(texture)$. S is the slope in degrees.

Global soil loss rates within IMAGE-GNM are estimated by adjusting soil erosion rates found within Europe based on slope, texture and land use[14]. Soil texture classes reduce or increase soil erodibility. Whilst coarse, very fine and peat soils have low erodibility of 0.5, medium and fine soil textures have increased erodibility. For the FF, slope and texture is considered within the FF whilst land use is considered within the emission inventory of an LCIA methodology. This is to ensure consistency of units within the LCIA method, whereby unit mass is considered within the emission inventory whilst time is considered within the FF.

Nutrient loads from erosion are a proportion of the total soil loss. For P, the IMAGE-GNM model keeps track of all inputs and outputs in the soil P budget. Hence historical tracking of P available in the soil is tracked from 1900, with initial stocks taken from Yang et al., (2013)[15]. We used soil P contents taken from 2000 within the IMAGE-GNM model. The soil P content for the year 2000 is reduced by subtracting the average nutrient balance for the year 1999 and 2000 and adding the average agricultural soil loss for 1999 and 2000; both taken from IMAGE GNM model results. This allowed us to obtain an initial P soil content to devise our erosional soil for specific crops within the main paper. N soil loss is solely related to soil loss through soil organic carbon (SOC) and N ratios.

For Phosphorus:

$$V_{Soilloss} = \frac{0.01 Soilloss(Landuse)}{BULK}$$

Where $V_{Soilloss}$ is the volume of soil loss in cubic meter per hectare, $Soilloss(Landuse)$ is the soil loss factors as per IMAGE-GNM in tonne per km^2 (See Appendix 2 for $Soilloss(Landuse)$ factors) and BULK is the soil bulk density measured in tonne per cubic metre. 0.01 is a conversion factor from km^2 to ha.

$$Density_{P\,Soil} = Pcontent \times 0.001/Depth_{topsoil}$$

Where $Density_{P\,Soil}$ is the P soil density in kg P/m^3, $Pcontent$ is the remaining mass balance of fertiliser plus existing P in the soil in grams of P per m^2. $Depth_{topsoil}$ is the depth of topsoil which is 0.3m. 0.001 converts grams of P per m^2 to kg P/m^2. Therefore, soilloss for P is:

$$Soilloss_P = V_{Soilloss} \times Density_{P\,Soil}$$

Where $Soilloss_P$ is the P soil loss in kg P per ha.

For Nitrogen:

$$Soilloss_N = \frac{SOC \times Soilloss(Landuse) \times 0.01 \times 1000}{C{:}N(Landuse)}$$

Where $Soilloss_N$ is the N soil loss in Kg N per ha, SOC is the soil organic carbon content fraction, $C{:}N(Landuse)$ is the carbon to nitrogen ratio which varies for land use (see Appendix 2).

1.2.3 Leaching ($f_{leach,soil}$)

$$f_{leach,soil} = [1 - MIN[(f_{climate} + f_{text} + f_{drain} + f_{soc}),1)]]f_{landuse}$$

The fraction of N lost by denitrification ($f_{den,soil}$) complements $f_{leach,soil}$ $\left(f_{den,soil} = 1 - f_{leach,soil}\right)$. Leaching fraction is related to soil texture (f_{text}), aeration (f_{drain}) and soil organic carbon (C) content (f_{soc})[16] (Appendix 2). Fine textured soils are more susceptible to reach and maintain anoxia, which favours denitrification as they are characterised by high capillary pressures and hold water more tightly than sandy soils. Denitrification rates tend to be higher in poorly drained soils[17]. The soil organic C content is used as a proxy for supply, which can have direct impact on the soil oxygen concentrations. $F_{landuse}$ is the land use effect on leaching whereby arable land has a value of 1, and grassland and natural vegetation has a value of 0.36[18] . The factor $f_{climate}$ combines the effects of temperature, water residence time, and NO_3 in the root zone on denitrification rates:

$$f_{climate} = f_K T_{RZ}$$

Where f_K is the temperature effect using the Arrhenius equation[19,20]:

$$f_K = 7.94 \times 10^{12} \exp\left(\frac{-E_{a,d}}{Rm\ K}\right)$$

Where $E_{a,d}$ is the activation energy (78430 J mol^{-1}), K the mean annual temperature (Kelvin) and Rm is the molar gas constant (8.3144 J $mol^{-1}K^{-1}$). T_{RZ} is calculated via:

$$T_{RZ} = \frac{AWC}{Q_{eff}}$$

Where AWC (m) is the available water capacity for the top 1m of soil and Q_{eff} is the total recharge rate (m/yr). AWC was taken from the IRSIC-WISE Soil database[9] and Q_{eff} was calculated based on the PCR-GLOBWB 2[10] Hydrological Model for precipitation input circa 2000.

1.2.4 Steady State Shallow Groundwater Fraction ($f_{SS\ shallow,gw}$)

The shallow groundwater fraction, $f_{shallow,gw}$, represents the steady state fraction of the total output from the shallow aquifer into surface water systems[8]:

$$f_{shallow,gw} = f_{Qint} \times DC_{shallow}$$

$$f_{Qint} = 1 - f_{Qgwb}$$

$$DC_{shallow} = \frac{1}{1 + k \times Tr}$$

Where f_{Qint} is the fraction of excess water delivered to the shallow aquifer devised from the partition ratio f_{Qgwb} of excess water flow between the shallow and deep aquifer. DC represents the delivery coefficient of nutrients under steady state assumptions, derived analytically for a homogenous and mixed system, where k represents the degradation rate coefficient and Tr represents the time of residence. The decay rate, k, is obtained via the half-life of nitrate ($dt50_{den}$) due to dentification[21]:

$$k = \frac{\ln(2)}{dt50_{den}}$$

Siliciclastic material exhibits low $dt50_{den}$ values of 1yr$^{-1,}$ whereas alluvial material has a $dt50_{den}$ value of 2 yr^{-1} and all other lithology classes have a $dt50_{den}$ value of 5yr^{-1}. Time of residence, T_r (years), is derived by estimating the (D) depth to groundwater and nitrate velocity. Global groundwater table depths are estimated by de Graff et al., (2017)[11] and implemented in PCR-GLBWB 2 at the 5 arc min:

$$Tr = MIN\left[\frac{pD}{R}, 1000\right]$$

Where R is the recharge rate (m year^{-1}) and p is the effective porosity (dimensionless). Global recharge rates are estimated by the PCR-GLOBWB 2[10]. Within IMAGE-GNM, the shallow aquifer is represented by a 5m thick layer and is subject to denitrification during transportation along the various flow paths in a homogenous and isotropic aquifer.

1.2.5 Steady State Deep Groundwater Fraction ($f_{SS\ deep,gw}$)

The deep groundwater fraction again represents the steady state input of nutrients from the deep groundwater into surface water systems from the total balance of nitrogen left on the field as within IMAGE-GNM model:

$$f_{deep,gw} = fQgwb \times DC_{shallow} \times DC_{deep}$$

Where DC_{deep} is the delivery coefficient for the deep groundwater aquifer. Denitrification is not considered to occur in the deep aquifer, therefore $DC_{deep} = 1$[8].

1.2.6 Submarine Groundwater Discharge (SGD) ($f_{Shallow,SGD}$, $f_{Deep,SGD}$)

SGD assumes a proportion of nitrogen load in groundwater is discharged directly to marine environments for cells adjacent to the coastline. The SGD fraction for shallow groundwater ($f_{Shallow,SGD}$) is 0.1, whilst for deep groundwater ($f_{Deep,SGD}$) the value equals 1.0. SGD is considered on all cells within 0 and 60km of the coastline.

1.2.7 Riparian Zone Reduction Fraction ($f_{den,rip}$)

A fraction of the shallow groundwater N load travels through the riparian zone ($f_{non-bypass}$). This fraction is determined by the fraction of the cell without a waterbody. The fraction with a waterbody represents the bypass fraction of the shallow groundwater N load that discharges directly into rivers (f_{bypass}).

Geochemical processes in the riparian zone require detailed hydrological and geographical information at very high spatial scales. Even at 0.1km resolution the topography of the riparian area cannot be adequately assessed. IMAGE-GNM therefore uses a conceptual approach whereby only the shallow groundwater input to the riparian zones is subject to denitrification and depends on local pH, temperature, water saturation, NO_3 availability and soil organic carbon availability[22,23]. As with soil denitrification, riparian zone denitrification is calculated using the dimensionless reduction factor:

$$f_{den,rip} = MIN[(f_{climate} + f_{text} + f_{drain} + f_{soc}),1)]f_{denpH,rip}$$

Where $f_{climate}$ is the product of f_K, temperature effect, water and NO_3 travel time through the riparian zone ($T_{r,rip}$). $T_{r,rip}$ depends on the thickness of the riparian zone (D_{rip}), available water capacity for the top 1m of the riparian zone ($tawc$) and on the flow of water entering the riparian zone from the shallow groundwater aquifer (q_{int}):

$$T_{r,rip} = \frac{D_{rip}tawc}{q_{int}}$$

1.2.8 Historical Fertiliser Transient State Fraction ($f_{N,TS/SS}$)

For the inclusion of historical transient state flows (i.e., historically varying fertiliser inputs) we used IMAGE-GNM historical nutrient inputs disaggregated from 30 arcmin to 5 arcmin resolution.

In transient state flows, the vertical flow distribution for the shallow system is uniform, therefore travel time is equal to mean travel time[8]. However, travel times for lateral flows to fluvial systems vary considerably. The travel time distribution for lateral flows is represented through the age of the groundwater at a specific depth:

$$g_{age}(z) = -Tr \times \ln(1 - \frac{z}{D})$$

Where g_{age} (yr) is the age of groundwater at a specific depth (z). The effects of denitrification in N leaching load at time t and depth z (($L_N(t, z)$) is represented through a first order degradation reaction and an exponential decay equation:

$$L_{N,TS,River} = L_N(t - g_{age}(z), 0)e^{-k\, g_{age}(z)}$$

Where t is time and k is the decay rate as described in steady state.

To develop a reduction or increase fraction that represents the varying historical fertiliser inputs, we divided total transient state loads by steady state loads for each grid cell:

$$f_{N,TS/SS} = \frac{L_{N,TS,River/Marine}}{L_{N,SS,River/Marine}}$$

1.2.9 In-Stream Nutrient Retention($\boldsymbol{R}$) and Subgrid Retention ($\boldsymbol{R_{Subgrid}}$)

The process of denitrification, sedimentation and uptake by aquatic plants contribute to N retention. Denitrification is generally the major component of N retention[24]. P is removed by sedimentation and sorption by sediment[25]. The IMAGE-GNM calculates retention as a first order approximation according to:

$$R = 1 - exp\left(\frac{v_{f,E}}{H_L}\right)$$

Where R is the fraction of nutrient load removed, $v_{f,E}$ is the net uptake velocity (m yr^{-1}) relating to nutrient E (N or P), and H_L is the hydraulic load (m yr^{-1}) obtained from:

$$H_L = \frac{D}{\tau}$$

Where D is the depth of waterbody (m), τ is the residence time (yr) calculated by:

$$\tau = \frac{V}{Q}$$

V is the waterbody volume (m^3) and Q is the discharge (m^3 yr^{-1}) for all waterbodies, except for river channels and floodplains where the discharge Q is reduced by the water volume in the floodplains (Q_f):

$$\tau = \frac{V}{Q - Q_f}$$

The Hydraulic Load (H_L) relates to removal through hydrological processes and the net uptake velocity ($v_{f,E}$), relates to removal from biological and chemical processes. Net uptake velocity is different for each element E (N or P). For N, the basic value for all water body types is 35m yr^{-1}, modified by temperature and N concentration[26].

$$v_{f,N} = 35\, f(t) f(C_N)$$

Where t is annual mean temperature (°C) and C_N is the N concentration in the water. $f(C_N)$ describes the effect of concentration on denitrification as a result of electron donor limitation in the case of high N loads. We interpolated, as conducted by Beusen et al., (2015), whereby $f(C_N)$is 7.2 for C_N = 0.0001 mg L−1 and $f(C_N)$ is 1 for C_N = 1 mg L−1, a further decrease to 0.37 $f(C_N)$is for C_N = 100mg L−1. N concentration in water is taken from IMAGE-GNM and equally disaggregated from 30arcmin to 5 arcmin.

A temperature effect $f(t)$ is used in the calculation of v_{fE} formed by:

$$f(t) = \alpha^{t-20}(t-20)$$

Where α = 1.0717 for N[27] and α = 1.06 for P[28]. For P the basic value for v_f is 44.5 myr^{-1} and again this is modified based on the temperature effect[28].

The subgrid retention fraction ($R_{Subgrid}$) is considered before retention at the grid cell level for all cells which do not have a lake or reservoir. Here we follow the parameterization method of lower-order streams following the approach by Wolheim et al., (2006)[26] and presented by Beusen et al., (2015)[8]. Subgrid retention fraction removes nutrient load from rivers below stream orders of 6 found within each grid cell that is not a lake or reservoir. Once subgrid retention is removed, grid cell retention and global load accumulation is devised. The final subgrid retention fraction ($R_{Subgrid}$) of stream orders 1 – 6, is the difference between original input load for the first order stream minus the input from the sixth order stream:

$$R_{Subgrid} = \frac{(Load_{in}^{1st} - Load_{in}^{6th})}{Load_{in}^{1st}}$$

1.3 Persistence Rate, λ

The persistence in a freshwater grid cell j or a Large Marine Ecosystem (LME) is the inverse sum of removal rates by hydrological (advection, $\lambda_{Adv\,E(j)}$) and biological and chemical processes ($\lambda_{Rent,E(j)}$):

$$\lambda_{E(j)} = \frac{1}{\lambda_{Adv\,E(j)} + \lambda_{Rent,E(j)}}$$

For freshwater environments, λ_{Adv} corresponds to the residence time τ of the hydrological load, which is formed by dividing the volume V (m^3) of the water body by the discharge Q (m^3yr^{-1}), taken from PCR-GLOBWB 2[10] for freshwater environments. For LMEs, Cosme et al., (2018)[6] provides water residence times for 66 LMEs devised from a literature review.

The persistence of net uptake velocities relating to biological and chemical processes (λ_{Rent}) in freshwater is calculated by dividing the net uptake velocity v_{fE}(myr^{-1}) by the depth D (m) of the water body (rivers, lakes and reservoirs).

$$\lambda_{Rent} = \frac{v_{fE}}{D}$$

For LMEs, nitrogen denitrification rates vary with geography and over time[29]. This study used Cosme et al., (2018)[6] results via a modelling approach to devise spatially variable denitrification rates across the 66 LMEs. The effect of time and space may be represented through an empirical relationship between nitrogen removal as a function of water residence time (months) in estuaries, river reaches, lakes, and continental shelf:

$$DIN_{rem,k} = 23.4 \times \tau\tau_l^{0.204}$$

The LME(l) – dependent denitrification rate constant ($\lambda_{\text{denitr},l}$) is determined using a first order removal equation, with t set to 1 year for the annual time integration, as per Cosme et al., (2018)[6]:

$$DIN_{rem,l} = e^{-\lambda\,\text{denitr}\,,l\,x\,t} \Leftrightarrow \lambda\,\text{denitr}\,,\,l = -\frac{\ln DIN_{rem,l}}{t}$$

1.4 Assumptions

Groundwater – IMAGE-GNM assumes a constant groundwater thickness for the shallow aquifer (D_{sgrw} = 5m) and for the deep aquifer (D_{dgrw} = 50m) following Meirnardi, (1994)[30]. In contrast, this study provides spatially-explicit groundwater thickness using data from PCR-GLOBWB 2[10], following aquifer thickness and distance to groundwater table researched by de Graff et al., (2017)[11].

Under the assumptions of IMAGE-GNM, the soil profile exists for 1 meter below the ground level[8]. The shallow groundwater aquifer exists up to 6 meters below the ground surface. Therefore, we assume a shallow aquifer is present at depths between 0 - 6 meters below ground level:

$$D_{sgrw} = \max\,(0.0, 6 - d_{gwT})$$

The deep aquifer lies between 6 and 56 meters below ground. The deep aquifer thickness is the difference between the overall ground thickness (D_{gw}) and the shallow aquifer thickness.

$$D_{dgrw} = \min\,(56, D_{gw} - D_{sgrw})$$

If the depth to groundwater is greater than 6 meters, only the deep groundwater aquifer exists. If the depth to groundwater table is greater than 56 meters, neither the shallow nor deep aquifer exists, and nutrients are assumed to be stored within the vadose zone. For continuity, regions where the deep aquifer exists, we assume all nutrients flow towards surface water bodies.

1.5 Aggregation:

Individual cell (i) FFs can be aggregated to larger spatial resolution (e.g., country, basin) to meet research requirements and address data and model constraints. Here we aggregated our FF data based on IMAGE-GNM diffusive emissions (DE) of N and P from all soils (arable, grassland and natural land) using the following equation:

$$FF_{i,LSR} = \frac{\sum_{LSR}(FF_{i,LSR}\;x\;DE_{i,LSR})}{\sum_{LSR}\;DE_{i,LSR}}$$

We provide resampled diffusive emissions from IMAGE-GNM and boundary shape files to preform aggregation of the FF to larger spatial resolutions.

1.6 Fate Factor Model Emissions Validation

For the comparison of the IMAGE-GNM model against our FF model for emissions, we used the percentage root mean squared error (PRMSE) as per Beusen et al., (2015)[8]. PRSME is calculated as:

$$PRMSE = \frac{100}{\bar{O}} \sqrt{\frac{\sum_{i=1}^{n}(O_i - M_i)^2}{n}}$$

Where $\bar{O}$ is the mean of the IMAGE-GNM results, O_i is the IMAGE-GNM result at cell *i*, M_i is the FF model simulated result at cell *i*. *n* is the number of grid cells with values greater than 0. As per Beusen et al., (2015), we consider PRSME values of less than 50% acceptable in view of the global scale of the model[8].

To validate our FF emission fractions against IMAGE-GNM model results we calculated the total emission of N & P via each emission pathway using IMAGE-GNM nutrient inputs. To allow for comparability to IMAGE-GNM 30 arcmin resolution, the simulated 5 arcmin emissions were sum aggregated to the 30 arcmin resolution. Where nutrient inputs required classification of landcover (surface runoff and erosional process) we solely validated our emissions from arable (cropland) cells, given our specific interest in crops for this study. Although we have additionally devised the FFs for grasslands, natural lands and direct emissions, we have not validated these against IMAGE-GNM as it is deemed out of scope for this study.

We compared simulated nutrient emissions to IMAGE-GNM nutrient emissions via:

1. Arable field emissions using IMAGE-GNM[8] nutrient inputs and Earthstat[31,32] nutrient inputs for surface runoff, erosional soil loss and leaching.
2. Historical groundwater load and effects from denitrification in the riparian zone using IMAGE-GNM[8] historical nutrient inputs solely.
3. Accumulated load after retention in rivers, based on IMAGE-GNM nutrient loads found in rivers after exportation from land cell compartments.

Points 2. and 3. used only IMAGE-GNM inputs as EarthStat data only provides arable nutrient inputs for the year 2000, hence the historical groundwater load and accumulated retention river load are incomparable.

2 Results

2.1 Comparison of FF Model Nutrient Loads against IMAGE GNM

2.1.1 Surface Runoff, Erosion and Leaching

We compared simulated nutrient emissions to IMAGE-GNM model's nutrient emission outputs (figure 2 and table 2). We ran our simulation firstly using nutrient inputs from IMAGE-GNM solely and latterly using nutrient inputs for the year 2000 from EarthStat[31,32]. For pre-existing nutrients found in soils for N and P in groundwater (under steady and transient state modelling), we used nutrient inputs taken from IMAGE-GNM[8].

Using nutrient inputs from IMAGE-GNM, model performance for erosional nutrient loss showed the best model similarity (PRMSE = 6.8% in N & 3.8% in P), followed by N leaching (PRSME = 6.9%) and surface runoff (PRSME = 9.8% in N & 10% in P). Erosion for N & P showed very slight overestimation noted in the residual plots clustering below 0. We attributed this slight overestimation due to an increased estimation of soil loss. Using nutrient inputs from Earthstat, all pathways (surface runoff, erosional and leaching) PRMSE performance ranged between 15% and 30%. Naturally, PRMSE values are higher using nutrient input data from Earthstat than IMAGE GNM given the majority of datasets (both nutrient input and model parameter datasets) are from improved data sources at the 5 arcmin resolution. Using Earthstat inputs, surface water runoff and erosion showed underestimation particularly for lower values of N and P. Slight under estimation in leaching is identified with no clear trend.

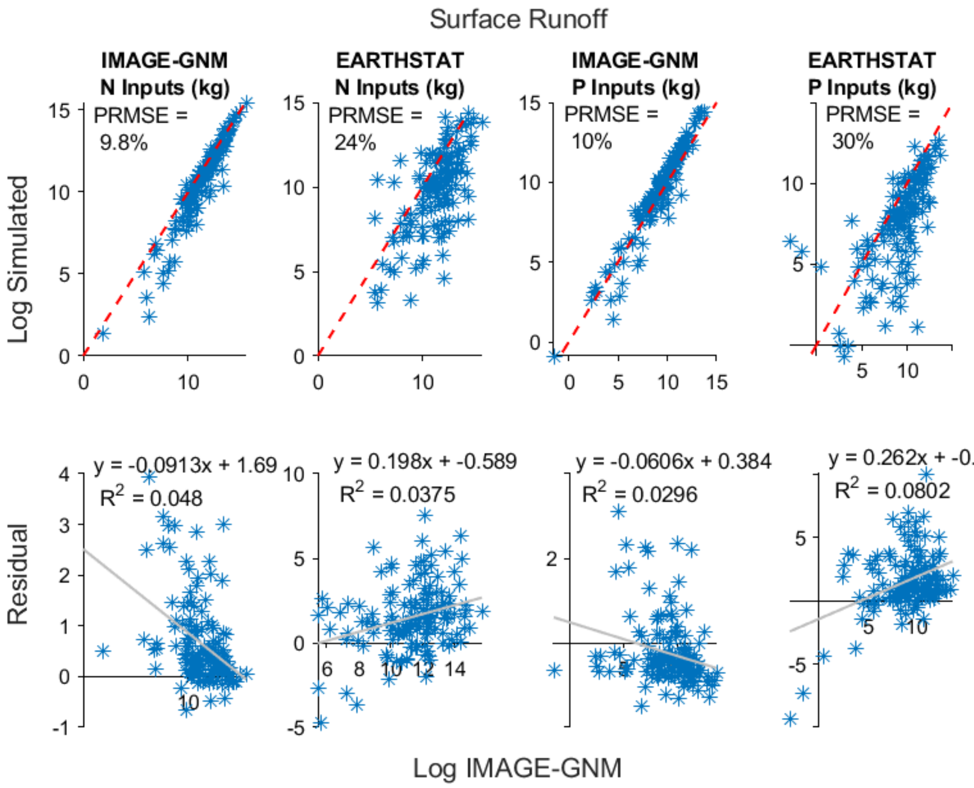

a.

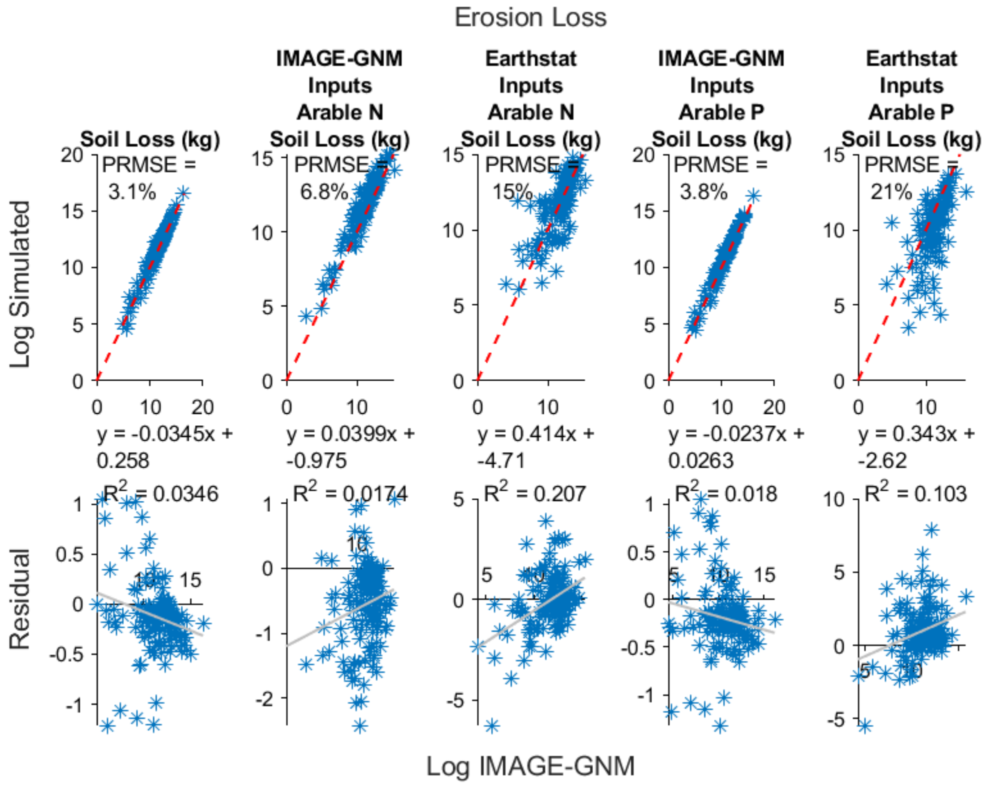

b.

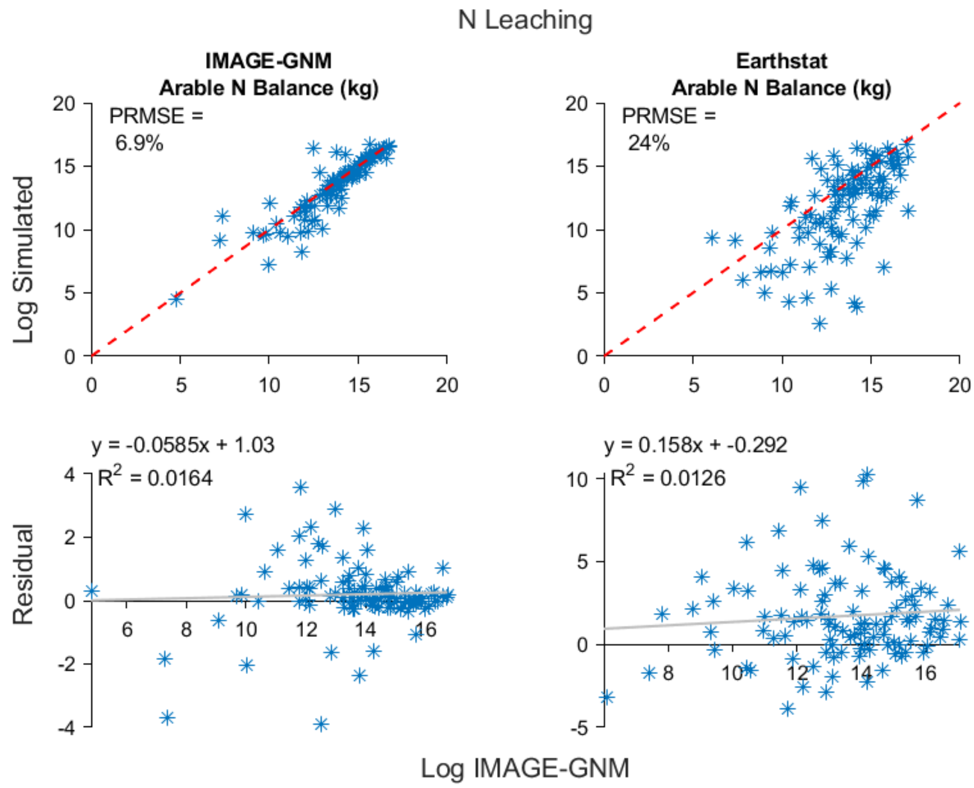

c.

Figure 2: Top graphs for each pathway (a. runoff, b. erosion, c. N leaching) represent the global comparison of log (simulated) and log (IMAGE GNM modelled) outputs with 1:1 lines. The bottom graph for each pathway represents global residual plots (log(simulated) minus log (IMAGE GNM modelled)) vs. (log(IMAGE GNM modelled)) with regression lines.

Comparing the global totals (table 2.), total nutrient outputs to rivers compared to total nutrient inputs to fields ratios (TN_{out}/TN_{in} & TP_{OUT}/TP_{IN}) showed an increase in N and reduction in P ratios using Earthstat nutrient inputs when compared to IMAGE GNM inputs. In comparing the individual pathways, reduced ratios were seen for surface runoff, however, increased ratios were identified for erosional and leaching pathways for N and P. Ratio differences are due to differences in crop numbers, global crop area, reduced nutrient inputs and variations in the local environmental characteristics found at the 5 arcmin resolution compared to the 30 arcmin.

Leaching to rivers identifies the quantity of leached N that is delivered to rivers through groundwater. Here the delivery fractions through the shallow, deep and submarine groundwater discharge (SGD) are used to estimate the load reaching rivers. We also applied a Transient State/Steady State (TS/SS) fraction to include the implications of historical fertiliser inputs. Our estimates of leaching to rivers are slightly higher than in IMAGE GNM. We attribute this to varying groundwater levels which reduce the time of residence and hence denitrification of nitrogen in the groundwater system. Additionally, we identified much higher porosity values using Gleeson et al., (2014)[12], which transfers greater quantities of nitrogen to the deep groundwater where denitrification does not occur, increasing delivery to rivers over time. Hence, we identified greater deep groundwater loads and higher SGD values (table 3).

Table 2: Represents global total comparisons for simulated results against IMAGE GNM modelled results. Here we sum the global total inputs and outputs for arable soils during the year 2000. Inputs represent nutrient inputs added to the fields and are not already existing on the field. Nutrient outputs represent the emission from the field edge (i.e. does not consider historical groundwater).

	IMAGE GNM Global Nutrient Totals for Land Pathways reaching rivers from for arable soils					This Study's Global Nutrient Totals for Land Pathways reaching rivers from for arable soils. Using data from Earthstat Nutrient Input data for 2000 and historical data from IMAGE GNM				
Time period	**2000**					**2000**				
Number of crops	**18**					**17**				
Resolution	**30 Arcmin**					**5 Arcmin**				
Global Crop Area in 2000 (ha)	**1.52E+09**					**8.58E+08**				
All values are circa 2000	**Surface Water Runoff**	**Erosion**	**Leaching to groundwater**	**Leaching to Rivers**	**Total**	**Surface Water Runoff**	**Erosion**	**Leaching to groundwater**	**Leaching to Rivers**	**Total**
Soil loss (Tg yr^{-1})	~	**5.36**	~	~		~	**3.48**	~	~	
Nitrogen										
TN IN (Tg N yr^{-1})	**129.71**	~	**51.53**	**51.53**	**129.71**	**105.82**	~	**41.8**	**41.8**	**105.82**
TN OUT (Tg N yr^{-1})	**5.31**	**5.14**	**33.58**	**11.25**	**21.7**	**2.81**	**4.30**	**27.9**	**16.38**	**23.48**
TN_{out}/TN_{in}	**0.04**	~	**0.65**	**0.22**	**0.16**	**0.03**	~	**0.68**	**0.39**	**0.22**
Phosphorus										
TP IN (Tg P yr^{-1})	**19.8**	**3745**	~	~	**19.8**	**17.24**	**2025.4**	~	~	**17.24**
TP OUT (Tg N yr^{-1})	**0.88**	**3.27**	~	~	**4.15**	**0.51**	**2.18**	~	~	**2.69**
TP_{OUT}/TP_{IN}	**0.04**	**0.000872**	~	~	**0.21**	**0.03**	**0.0011**	~	~	**0.16**

2.1.2 Groundwater Steady State and Transient State

N Groundwater under steady state (SS) and transient state (TS) had PRMSE values ranging between 10% and 17% for the shallow, deep and SGD (figure 3).

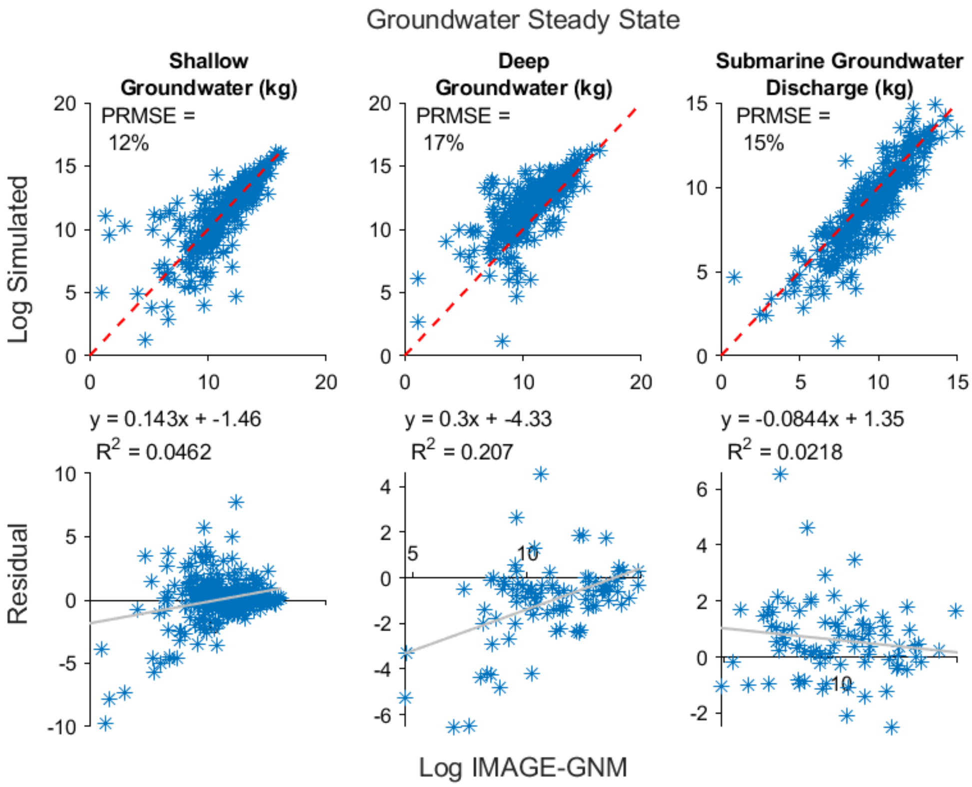

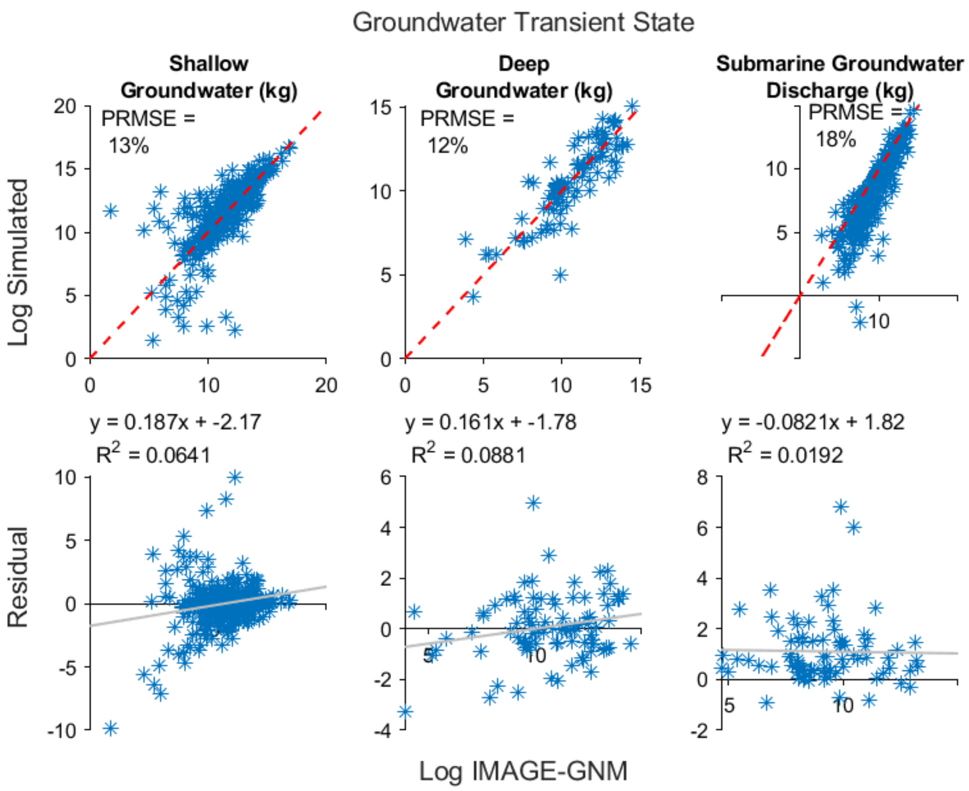

Figure 3: Top graphs for groundwater under steady (a.) and transient (b.) state assumptions represent the global comparison of log(simulated) and log(IMAGE GNM modelled) outputs with 1:1 lines. The bottom graph for each pathway represents global residual plots (log(simulated) minus log (IMAGE GNM modelled)) vs. (log(IMAGE GNM modelled)) with regression lines.

For all landcovers, the total N groundwater flow reaching streams and marine environments is 33.25 Tg, whilst in IMAGE the total quantity was 29.17 Tg under TS (table 3). This is to be expected as varying groundwater depth reduces the quantity of denitrification occurring in the shallow zone, hence increasing the nutrient outflow to rivers. TS showed a very slight reduction in the global total compared to SS in both IMAGE GNM and this study. This is due to varying historical fertiliser use where some regions have increased fertiliser use and others have decreased use over time. We devised a historical fertiliser factor by dividing the TS by SS to reduce or increase N loads to rivers depending on the historical load (table 3).

Table 3: Represents comparisons of the global total output of N load from groundwater for simulated results against IMAGE GNM modelled results under steady and transient states. N outputs represent the groundwater load reaching rivers from the field after leaching has occurred. Steady states consider nutrient leaching is constant over time whilst transient states consider the variable inputs of fertilisers through time. Nutrient inputs are taken solely from IMAGE GNM. For steady states N leaching inputs are from the year 2000. For transient states N leaching considers variable leaching rates dating back to 1700. Denitrification is considered to remove all N leaching 50 years after N is added to soils. TS/SS represent the division of transient state loads by steady state loads to devise the reduction or increase fractions to account for spatial historical fertiliser input differences. TS/SS histogram shows some regions increase in TS/SS fractions whilst others decrease. We applied a maximum increase fraction of 2 due to model uncertainty within groundwater.

	IMAGE GNM						**This Study**					
	Steady State			Transient State			Steady State			Transient State		
	Shallow	Deep	SGD	Shallow	Deep	SGD	Shallow	Deep	SGD	Shallow	Deep	SGD
TN OUT (Tg N yr⁻¹)	25.60	4.13	0.84	25.84	2.64	0.70	24.15	6.90	2.72	28.51	2.13	2.61
Total (Tg N yr⁻¹)	30.57			29.17			33.77			33.25		
TS/SS Global	0.95						0.98					
TS/SS Histogram	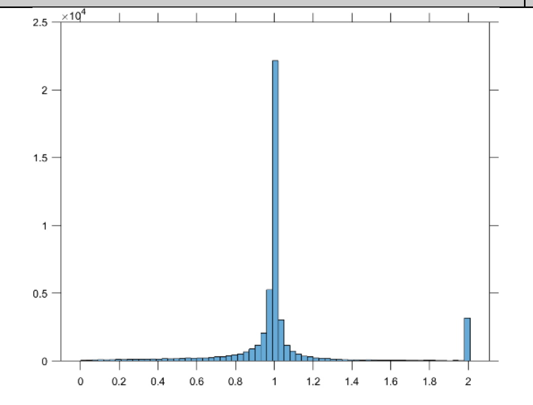						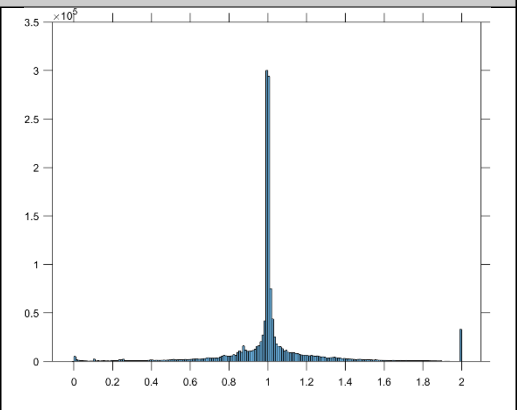					
TS/SS Map	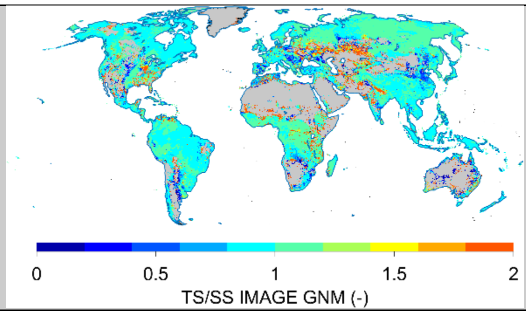						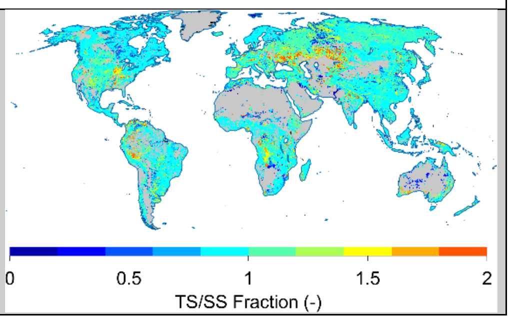					

2.1.3 Subgrid Retention and Accumulated River Load after Grid Retention

The subgrid retention load showed model PRSME in N as 16% and in P 14%. Subgrid nutrient retention load was slightly overestimated by our FF model (figure 4a.). Accumulated river nutrient load post grid retention showed the least model similarity (PRSME = 36% for N and 29% for P) (figure 4b.). Extreme overestimation was identified when IMAGE GNM predicts loads of less than 1kg. Spatially these were identified over arid regions where differences in water fractions, water volumes and surface water area at smaller resolutions impacted the hydraulic load; an input parameter to quantify retention. Disregarding simulated accumulation loads that are below 1kg in IMAGE GNM we saw model performance improved to PRSME = 14% for N and 17% for P (figure 4b). Hence, we recommend caution for use of FF model results over arid regions.

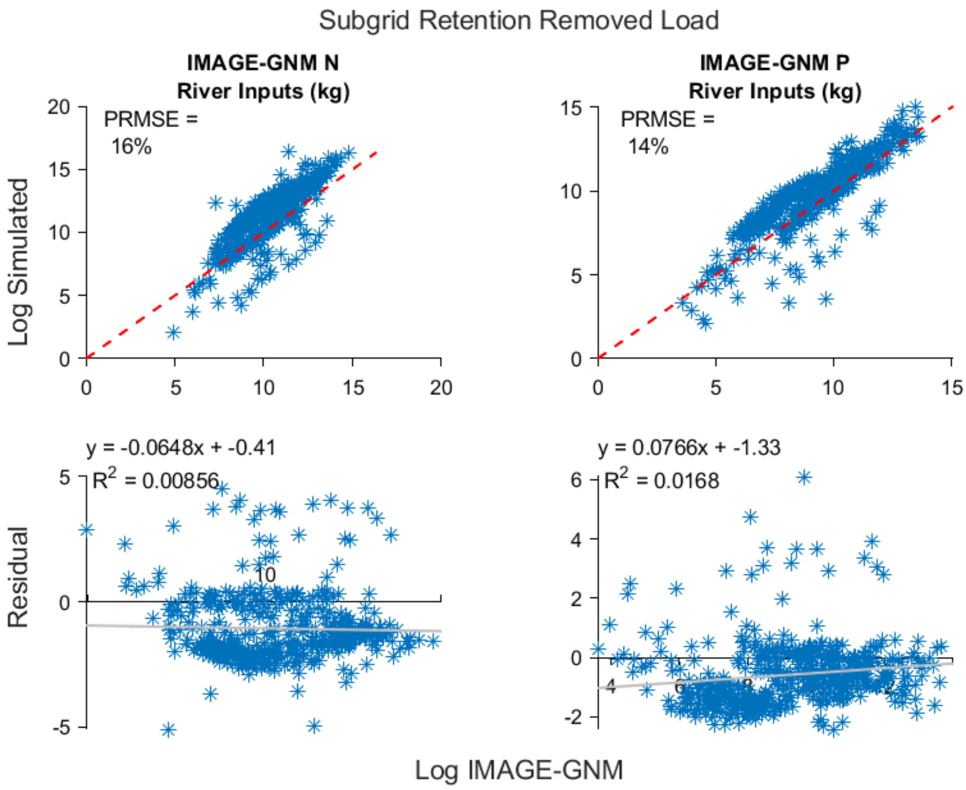

a.

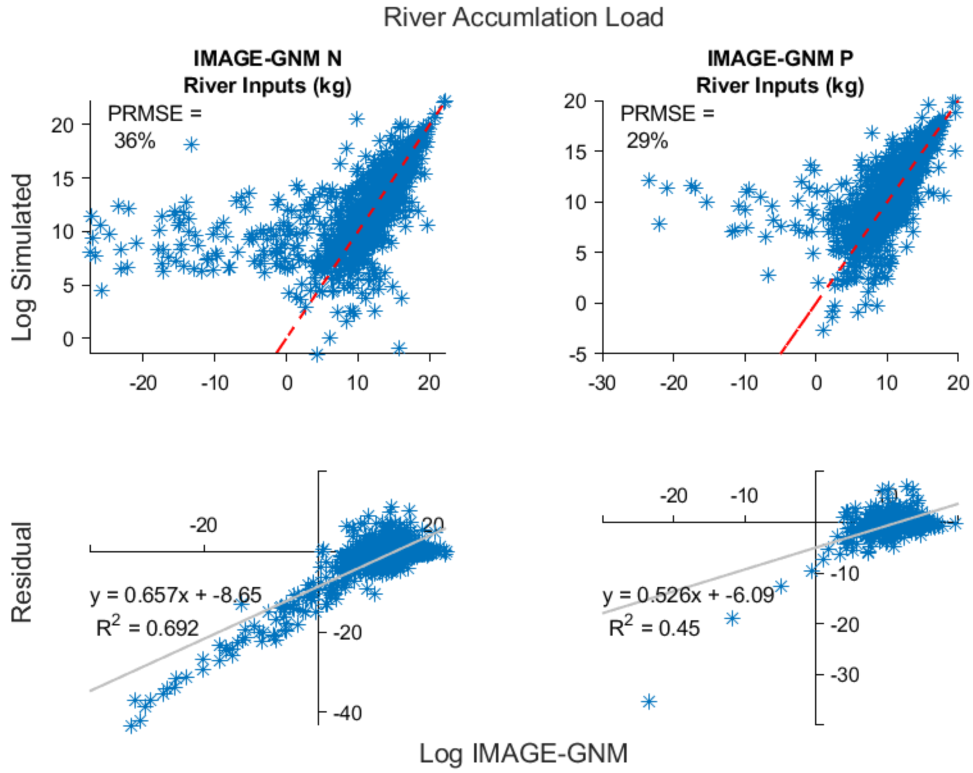

b.

Figure 4: Top graphs for subgrid retention removed load (a.) and river accumulation load (b.) representing the global comparison of log (simulated) and log (IMAGE GNM modelled) outputs with 1:1 lines. The bottom graph for retention loads represent global residual plots (log(simulated) minus log (IMAGE GNM modelled)) vs. (log(IMAGE GNM modelled)) with regression lines. Nutrient inputs are taken from IMAGE GNM solely for model validation.

2.2 Fate Factor Model Results

The summary of statistics of the spatial distribution of the fate factor at the global scale is presented in table 4. The Fate Factor (FF) results for all land covers (arable, grassland and natural) and soil emission pathways (surface runoff, erosion and leaching) are shown in Figure 5. The results discussed are for diffusive soil emissions solely for N and P to freshwater and N to marine environments. Although our results represent diffusive emissions, direct emissions to river and marine FFs can be found within the raster data files. Direct emissions had to be calculated as part of the diffusive emission calculation. FFs for all soils at the grid cell are a weighted average (weighted by nutrient emissions from IMAGE GNM[8]) of the land use fraction (e.g arable, grassland and natural).

Table 4: Statistics of distribution of fate factors (days) results for all emission routes to freshwater and marine environments

Statistics	**Fate Factor (days) per nutrient and receptor waterbody type**		
	Freshwater N	Freshwater P	Marine N
Minimum	9.80E-22	6.81E-22	5.11E-43
5th Percentile	7.10E-04	7.34E-04	1.12E-06
Mean	5.24	2.99	26.54
95th percentile	10.50	8.18	119.41
Maximum	70417.88	40126.06	3977.53
Spatial variability	174.03	68.13	96.68

Under the assumption of the limiting nutrient concept[33], we assessed the inflection point used by Helmes et al., (2012)[2] to detect the difference between longer and shorter FF persistence values for all land cover types (figure 5 b,c,d). The inflection point identifies emissions with short and long travel times to the river mouth or near marine ecosystem. Inflection for P and N in freshwater is 0.056 days and 0.084 days, respectively. For marine environments, N inflection increased to 5.45 days.

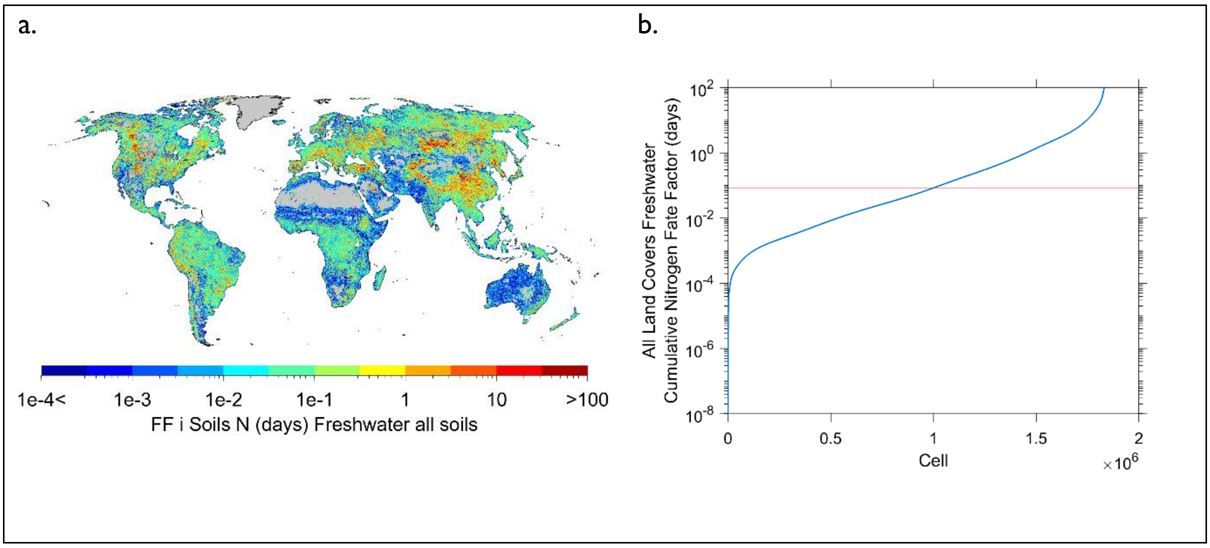

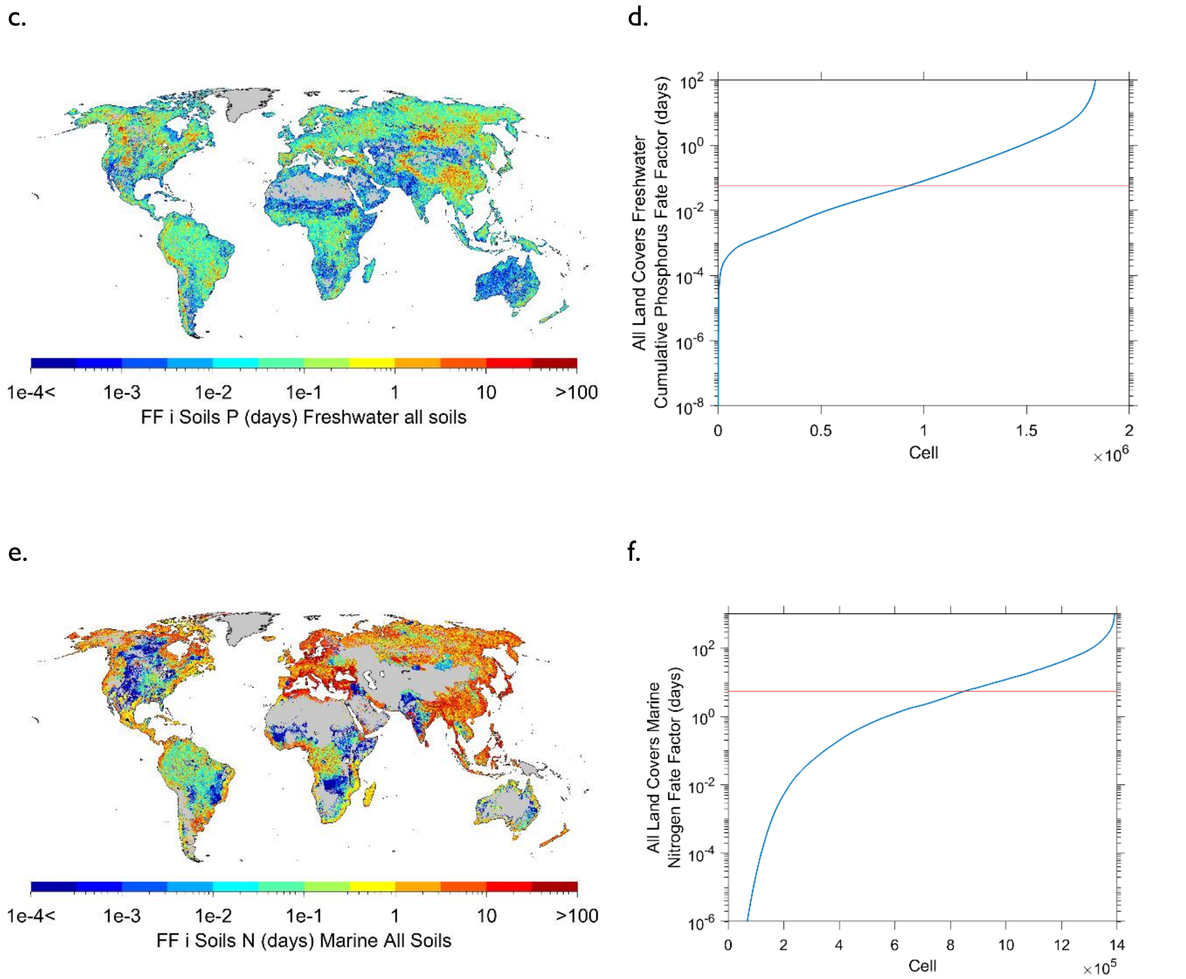

Figure 5: Fresh and marine water FFs for all land uses (agricultural, grassland and natural). The cumulative FF represents the cumulative persistence of nutrients (N and P) from soils in freshwater, from the point of emission to the river mouth for the year 2000 (a. & c.). The FF for marine environments is not cumulative and represents the persistence of the fraction of emission within a Large Marine Ecosystem (LMEs) (e.). Greyscale coloured grid cells identify land covers such as ice caps and deserts and have no available FFs. In the case of marine FFs, greyscale identifies those regions which do not connect to a marine environment. Ranked cumulative FFs for N and P in freshwater for all land covers (arable, grassland and natural) are shown in b. and d. respectively. Ranked FFs for N in marine environments for all land covers (arable, grassland and natural) are shown in subplot f. The inflection line (red) identifies emissions with short and long travel times to the river mouth or near marine ecosystem. Inflection for P and N in freshwater is 0.056 days and 0.084 days, respectively. For marine environments, nitrogen inflection increased to 5.45 days.

2.3 Comparison with other Fate Factor studies

To implement a more robust comparison to previous studies, we compared the diffusive and direct emission FFs formulated in this study to previous research (table 5). Although direct emission FFs are not a focus of this study, direct emission FFs had to be formulated before estimating diffusive emission FFs.

Direct emission FFs were assumed to be within rivers of stream order six and above. Therefore, subgrid retention was not considered for direct emission FFs. We assumed that stream orders lower than six would be too small for effluent nutrient discharge. Additionally, we aggregated FFs by their respective emission inventories (diffusive emissions for soils and direct emissions to rivers). Emission inventory data for diffusive and direct were both taken from IMAGE-GNM[8].

The FF model presented here, derives spatially explicit FFs for N and P at the global scale from soils and direct emissions using a single methodology at the 5 arcmin resolution. Until recently, global FFs had only been estimated individually for P in freshwater[2] and N in marine environments[6]. However, Payen et al., (2021) recently developed global FFs for N and P for freshwater environments at the basin scale[34]. Additionally, Zhou et al., (2022) developed global FFs for N to freshwater for direct and diffusive emissions based on IMAGE GNM model[35]. Here, our research is the first to derive comparable FFs to all previous global FFs, devised for N and P, in freshwater and marine environments, for direct and diffusive sources, within a single study (table 5).

Table 5: Globally aggregated weighted-emission Fate and Characterisation Factors. Land cover fractions are taken from PCR-GLOBWB 2 for the purpose of continuity for modelling within the supplementary material. Within the main paper we took land cover fractions from Monfreda et al., (2008)[36].

Fate Factors (days)

	Zhou et al., (2022)[35]		Payen et al (2021)[34]		Helmes et al. (2012)[2]	Cosme et al. (2018)[6]		**This study**				
Resolution	30 arcmin		Basin		30 arcmin	Basin		**5 arcmin**				
Emission Source	Diffusive (excluding erosions)	Direct	Soils (Diffusive Sources)	Point Sources	Point Sources	Diffusive	Direct	**Arable Soils**	**Grassland Soils**	**Natural Soils**	**Diffusive (All Soils)**	**Direct**
Marine (Nitrogen)	~	~	~			43.8	96	**19.53**	**40.60**	**28.33**	**34.46**	**94.30**
Freshwater (Phosphorus)			23	247	130			**4.78**	**4.95**	**5.05**	**5.38**	**6.53**
Freshwater (Nitrogen)	6.7*	29.3	125	257	~			**8.42**	**6.43**	**6.30**	**7.40**	**23.25**

* Note: diffusive weighted average. Just the average was provided across all cells for diffusive sources.

Our FF results were lower than all previously predicted FFs for direct and diffusive emission sources. For direct emissions, whilst N marine FFs were within a 5% range predicted by Cosme et al., (2018)[6], N and P freshwater FFs were an order of magnitude lower than values predicted by Payen et al., (2021)[34] and Helmes et al., (2012)[2]. However, our results compared well and were within range with the Zhou et al., (2022)[35] study for N FFs in freshwater. For diffusive emissions, whilst previous LCIA methodologies have suggested diffusive emissions are roughly 10% of direct FF emissions[2,37], some LCIA methods have not made any deductions for diffusive emissions[38]. Our results show for marine environments, diffusive emission FFs are 36.5% of direct N emission FFs and for freshwater are 31.8% for N and 82.4% for P. Cosme et al., (2018)[6] showed N diffusive emission FFs to marine environments were 45.6% of direct emission FFs. Payen et al., (2021)[34] showed diffusive emission FFs were 9.3% of direct emission FFs to freshwater for P and 48.6% of N. Zhou et al., (2022)[35] showed diffusive N emission FFs to freshwater were 22.8% of direct emission FFs. Our results showed strong similarities for the comparison of N diffusive to direct emissions with Cosme et al., (2018)[6] and Zhou et al., (2022)[35]. However, our study showed a weak percentage comparison of diffusive to direct emissions with Payen et al., (2021)[34].

We excepted the FF for freshwater environments to be smaller than the FF for marine environments, as rivers are natural transmission pathways for water, nutrients and sediments to oceans. Our N FF for freshwater is within a similar range for our P FF freshwater, providing further confidence in our predicted results. Greater FFs were found on arable land uses for N due to greater removal fractions (Appendix 2). However, for P higher FFs were identified on natural lands due to high erosion on steep slopes.

Our results varied with previous studies due to different: (1) nutrient models used for the basis of the FF (e.g. GLOBAL NEWS 2 Vs IMAGE GNM), (2) nutrient indicators assessed (e.g. dissolved inorganic nitrogen vs total nitrogen), (3) spatial resolutions (basin scale vs 30arc min vs 5 arcmin) and (4) FF model structures. Payen et al., (2021)[34] and Cosme et al., (2018)[6] predict their FFs at the watershed level using the Global NEWS 2 model for dissolved inorganic nutrients. Higher FFs predicted by both Payen et al., (2021)[34] and Cosme et al., (2018)[6] may be due to differences between Global NEWS 2 model and IMAGE GNM meaning lower total nitrogen was found by IMAGE GNM (37 Tg (N/yr) compared to Global NEWS2 (45 Tg N/yr). Fundamental differences exist between IMAGE GNM and GLOBAL NEWS 2 to stimulate N removal and transportation modelled within the terrestrial and aquatic systems. IMAGE-GNM provide predictive advantages by adding detailed modelling of land fate processes, which includes explicit groundwater denitrification in soils, aquifers and riparian zones, rather than regression models (Global NEWS 2[5]) that lump process behaviour within watersheds by export constants. Additionally, different hydrological and terrestrial data inputs and spatial resolutions exist between the two models.

Strong comparisons existed between Zhou et al., (2022)[35] and this study because the FFs are based on the IMAGE GNM model (either results or equations) and we adopted similar FF model structures for freshwater (cumulative FF). However, this study improved the FF model by:

1. Using updated 5 arcmin resolutions datasets for soil properties and hydrological data inputs.

2. Considering variations in groundwater depth and thickness globally on the N nutrient load discharged via groundwater.
3. Considering subgrid and grid level nutrient retention.
4. Using updated hydrological datasets through PCR-GLOBWB 2[10]; which includes water return flows for irrigation, not modelled in PCR-GLOBWB 1[7].
5. Estimating P in freshwater and N in marine environments for direct and diffusive emissions.
6. Developing an FF model from climate, soil and hydrological data to facilitate analysis of FFs under climate and land use change scenarios.

Overall, our results and previous studies suggest, the assumption that diffusive emissions are 10% of direct emission is not a sufficiently robust estimate for diffusive emission FFs. Additionally, large FF variations exist between studies, identifying the strong reliance on robust global nutrient models for FF model development.

2.4 User Information for the Fate Factor

Unlike in some previous FF models[2], here, the actual emission at the field is incorporated within our FF model ($FF_{soils\ E\ (w)\ (i)}$) with; E representing the nutrient type, being N or P; (*w*) representing the receiving waterbody, either freshwater (*fw*) or marine (*LME*); and (i) representing the emission pathways, either surface runoff, erosion or leaching. Therefore, our emissions inventory within an LCIA framework incorporates the nutrient inputs, soil loss and mass balance as per IMAGE-GNM. This makes formulating the emission inventory for LCIA practitioners easier. For surface water, the nutrient load within a receiving waterbody receptor via surface runoff is fed solely by the initial nutrient inputs on land for each nutrient type (E):

$$Load_{E\ (w)(Surface\ Runoff)} = Input_E \times FF_{E\ (w)\ (Surface\ Runoff)}$$

For erosion, P erosional processes consider the initial soil P content and any positive soil P mass balances left on the field. Within IMAGE-GNM, P soil content is assumed to vary over time due to historical fertiliser input. The natural P content baseline is taken from IMAGE GNM from the year 1900. The N erosional process considers the C:N ratio of the soil organic carbon content, which is assumed to be constant over time. To calculate soil loss load, we used natural soil loss as a baseline to reflect anthropogenic pressures causing a relative change from natural land to grassland or arable lands. FF differences between land uses are constant (C_{LD}) with values for N as 45.3046 and 2.4138 and for P as 38.6897 and 2.4138 for arable and grasslands, respectively:

$$Load_{E\ (w)\ (Erosion)} = \frac{(Soilloss_{E,Landuse} - Soilloss_{E,Natural\ 1900}) \times FF_{E\ (w)\ (Erosion)}}{C_{E\ LD} Soilloss_E \times FF_{E\ (w)\ (Erosion)}}$$

$$Load_{P,Fw,Erosion\ New} = P_{budget>0} \times FF_{P,Fw\ (Erosion)}$$

For subsurface transport only N is considered, as P is easily absorbed by soil minerals[8]. All N positive soil balances are subject to leaching and exclude the N lost by surface runoff:

$$N_{budget} = N_{budget} - (Input_E \times f_{qrso})$$

$$Load_{N,Fw/LME,Leaching} = N_{budget>0} \times FF_{N,Fw/LME\ (Leaching)}$$

Practitioners of the FF should use FFs for all soils if the land use is unknown or their data represents different land uses with unknown fractions. If land use is known, FFs for the corresponding land use and grid cell should be used. Practitioners should follow the guidance as per Payen et al., (2020) for variations in N limiting, P limiting or co-limiting regions. Payen et al., (2020) suggests if the limiting nutrient is unknown, one should assume a co-limiting system of N_{eq} and P_{eq} and aggregate using the Redfield Ratio to express $algae_{eq.}$ If the user wishes to distinctly identify different pathway routes, as within IMAGE-GNM, then the Fate Factor from a specific land use and transport pathway should be used with the corresponding emission inventory requirements. Use of specific transport pathway fate factors should follow emission inventory requirements as per IMAGE-GNM. Due to retention model validity, we suggest users should use the FF model with caution over natural lands with desert and mountainous geomorphic terrain.

We present FF characterisation for all land covers globally (i.e. assuming arable, grass or natural land can be found anywhere across the globe). In doing so, we support LCIA studies that may wish to identify fertiliser use impacts from land conversion. Furthermore, as no global FF factors are developed in transient state, the FFs presented here may in the future provide insight to regions of high fertiliser use impacts under the impacts of climate change. Studies have shown Canada and Russia will be prime agricultural countries under the impacts of climate change in years to come[39]. Our FF model identifies Russia as one of the highest regions for the transport of nutrients to fluvial and marine environments.

2.5 Conclusion and Furtherwork

This study presented the opportunity to develop a spatially-explicit FF at the 5 arcmin resolution based on IMAGE-GNM modelling concepts. Given the study's main purpose is to understand fertiliser impact from crop production at the 5 arcmin resolution, there are further developments that can be incorporated to make a more robust FF model using IMAGE-GNM. Here we present an FF model developed from climate, soil and hydrological datasets. As such, this presents an FF model which may be used to predict future FFs under climate and land use change scenarios. Secondly, we only validated our FF model for arable land emissions pathways; validation of grass and natural lands were deemed out of scope for this study. Lastly, the current FF model is complex in a practical sense. To support LCIA practitioners and the use of the FF model, a more simplified model that easily connects emission inventories to FF characterisations may enhance user ability. This will support the growing demand for spatially-explicit LCIA studies in recognition of the UN Sustainable Development Goals and transparency of product and services' impact on the environment.

3 Reference List

1. Rosenbaum, R. K., Margni, M. & Jolliet, O. A flexible matrix algebra framework for the multimedia multipathway modeling of emission to impacts. *Environ. Int.* **33**, 624–634 (2007).
2. Helmes, R. J. K., Huijbregts, M. A. J., Henderson, A. D. & Jolliet, O. Spatially explicit fate factors of phosphorous emissions to freshwater at the global scale. *Int. J. Life Cycle Assess.* **17**, 646–654 (2012).
3. Cosme, N. & Hauschild, M. Z. Characterization of waterborne nitrogen emissions for marine eutrophication modelling in life cycle impact assessment at the damage level and global scale. *Int. J. Life Cycle Assess.* **22**, 1558–1570 (2017).
4. Morelli, B. *et al.* Critical review of eutrophication models for life cycle assessment. *Environ. Sci. Technol.* **52**, 9562–9578 (2018).
5. Mayorga, E. *et al.* Global Nutrient Export from WaterSheds 2 (NEWS 2): Model development and implementation. *Environ. Model. Softw.* **25**, 837–853 (2010).
6. Cosme, N. M. D. Spatially explicit fate factors of waterborne nitrogen emissions at the global scale. *Int. J. Life Cycle Assess.* **23**, 1286–1296 (2018).
7. Global monthly water stress: 1. Water balance and water availability - van Beek - 2011 - Water Resources Research - Wiley Online Library. https://agupubs.onlinelibrary.wiley.com/doi/full/10.1029/2010WR009791.
8. Beusen, A. H. W., Van Beek, L. P. H., Bouwman, A. F., Mogollón, J. M. & Middelburg, J. J. Coupling global models for hydrology and nutrient loading to simulate nitrogen and phosphorus retention in surface water – description of IMAGE–GNM and analysis of performance. *Geosci. Model Dev.* **8**, 4045–4067 (2015).
9. Batjes, N. H. ISRIC-WISE derived soil properties on a 5 by 5 global grid (ver. 1.2). 56.
10. Sutanudjaja, E. H. *et al.* PCR-GLOBWB 2: a 5 arcmin global hydrological and water resources model. *Geosci. Model Dev.* **11**, 2429–2453 (2018).
11. de Graaf, I. E. M. *et al.* A global-scale two-layer transient groundwater model: Development and application to groundwater depletion. *Adv. Water Resour.* **102**, 53–67 (2017).
12. Gleeson, T., Moosdorf, N., Hartmann, J. & Beek, L. P. H. van. A glimpse beneath earth's surface: GLobal HYdrogeology MaPS (GLHYMPS) of permeability and porosity. *Geophys. Res. Lett.* **41**, 3891–3898 (2014).
13. Velthof, G. L., Oudendag, D. A. & Oenema, O. Development and application of the integrated nitrogen model. 102.
14. Cerdan, O. *et al.* Rates and spatial variations of soil erosion in Europe: A study based on erosion plot data. *Geomorphology* **122**, 167–177 (2010).
15. Yang, X., Post, W. M., Thornton, P. E. & Jain, A. The distribution of soil phosphorus for global biogeochemical modeling. *Biogeosciences* **10**, 2525–2537 (2013).

16. Drecht, G. V., Bouwman, A. F., Knoop, J. M., Beusen, A. H. W. & Meinardi, C. R. Global modeling of the fate of nitrogen from point and nonpoint sources in soils, groundwater, and surface water. *Glob. Biogeochem. Cycles* **17**, (2003).

17. Bouwman, A. F., Fung, I., Matthews, E. & John, J. Global analysis of the potential for N_2O production in natural soils. *Glob. Biogeochem. Cycles* **7**, 557–597 (1993).

18. Keuskamp, J. A., van Drecht, G. & Bouwman, A. F. European-scale modelling of groundwater denitrification and associated N2O production. *Environ. Pollut.* **165**, 67–76 (2012).

19. Firestone, M. K. Biological Denitrification. in *Nitrogen in Agricultural Soils* 289–326 (John Wiley & Sons, Ltd, 2015). doi:10.2134/agronmonogr22.c8.

20. Shaffer, M. J., Halvorson, A. D. & Pierce, F. J. Nitrate Leaching and Economic Analysis Package (NLEAP): Model Description and Application. in *Managing Nitrogen for Groundwater Quality and Farm Profitability* 285–322 (John Wiley & Sons, Ltd, 2015). doi:10.2136/1991.managingnitrogen.c13.

21. Lithologic composition of the Earth's continental surfaces derived from a new digital map emphasizing riverine material transfer - Dürr - 2005 - Global Biogeochemical Cycles - Wiley Online Library. https://agupubs.onlinelibrary.wiley.com/doi/10.1029/2005GB002515.

22. Denitrification. https://www.ncbi.nlm.nih.gov/pmc/articles/PMC373209/.

23. Šlmek, M. & Cooper, J. E. The influence of soil pH on denitrification: progress towards the understanding of this interaction over the last 50 years. *Eur. J. Soil Sci.* **53**, 345–354 (2002).

24. Saunders, D. L. & Kalff, J. Nitrogen retention in wetlands, lakes and rivers. *Hydrobiologia* **443**, 205–212 (2001).

25. Reddy, K. R., Kadlec, R. H., Flaig, E. & Gale, P. M. Phosphorus Retention in Streams and Wetlands: A Review. *Crit. Rev. Environ. Sci. Technol.* **29**, 83–146 (1999).

26. Wollheim, W. M., Vörösmarty, C. J., Peterson, B. J., Seitzinger, S. P. & Hopkinson, C. S. Relationship between river size and nutrient removal. *Geophys. Res. Lett.* **33**, (2006).

27. Wollheim, W. M. *et al.* Global N removal by freshwater aquatic systems using a spatially distributed, within-basin approach. *Glob. Biogeochem. Cycles* **22**, (2008).

28. Marcé, R. & Armengol, J. Modeling nutrient in-stream processes at the watershed scale using Nutrient Spiralling metrics. *Hydrol. Earth Syst. Sci. Discuss.* **6**, 501–533 (2009).

29. Seitzinger, S. *et al.* Denitrification Across Landscapes and Waterscapes: A Synthesis. *Ecol. Appl.* **16**, 2064–2090 (2006).

30. Meinardi, C. R. Groundwater recharge and travel times in the sandy regions of the Netherlands. (1994).

31. Mueller, N. D. *et al.* Closing yield gaps through nutrient and water management. *Nature* **490**, 254–257 (2012).

32. West, P. C. *et al.* Leverage points for improving global food security and the environment. *Science* **345**, 325–328 (2014).

33. Harris, G. P. The concept of limiting nutrients. in *Phytoplankton Ecology: Structure, Function and Fluctuation* (ed. Harris, G. P.) 137–165 (Springer Netherlands, 1986). doi:10.1007/978-94-009-3165-7_7.
34. Payen, S., Cosme, N. & Elliott, A. H. Freshwater eutrophication: spatially explicit fate factors for nitrogen and phosphorus emissions at the global scale. *Int. J. Life Cycle Assess.* (2021) doi:10.1007/s11367-020-01847-0.
35. Zhou, J., Scherer, L., van Bodegom, P. M., Beusen, A. & Mogollón, J. M. Regionalized nitrogen fate in freshwater systems on a global scale. *J. Ind. Ecol.* **n/a**,.
36. Monfreda, C., Ramankutty, N. & Foley, J. A. Farming the planet: 2. Geographic distribution of crop areas, yields, physiological types, and net primary production in the year 2000. *Glob. Biogeochem. Cycles* **22**, (2008).
37. ReCiPe2016v1.1. | RIVM. https://www.rivm.nl/documenten/recipe2016v11.
38. IMPACT World+. http://www.impactworldplus.org/en/presentation.php.
39. Hannah, L. *et al.* The environmental consequences of climate-driven agricultural frontiers. *PLOS ONE* **15**, e0228305 (2020).